Detecting volcano-related underground mass changes with a quantum gravimeter

Laura Antoni-Micollier[1], Daniele Carbone[2], Vincent Ménoret[1], Jean Lautier-Gaud[1], Thomas King[2], Filippo Greco[2], Alfio Messina[2], Danilo Contrafatto[2], and Bruno Desruelle[1]

[1]: iXblue, Institut d'Optique d'Aquitaine, 1 rue François Mitterrand, 33400 Talence, France

[2]: Istituto Nazionale di Geofisica e Vulcanologia, Sezione di Catania - Osservatorio Etneo, Catania, Italy

Corresponding author: Daniele Carbone (daniele.carbone@ingv.it)

Key Points:

- We present the world's first time series acquired with an absolute quantum gravimeter in the summit crater zone of an active volcano.
- Despite the unfavorable ambient conditions, the quantum gravimeter produced high quality data, allowing to track volcano-related changes.
- Comparison with the data from other gravimeters highlights changes due to bulk mass redistributions within Mt. Etna's feeding system

Abstract

We present the world's first time series acquired in the summit area of an active volcano with an absolute atom interferometry gravimeter. The device was installed ~2.5 km from the active craters of Mt. Etna volcano and produced a continuous high–quality gravity time series, despite the unfavorable environmental conditions at the installation site and the occurrence of phases of high volcanic tremor during the acquisition interval. Comparison with data from other gravimeters installed elsewhere on Mt. Etna highlights correlated anomalies, demonstrating that the quantum device measured gravity variations driven by bulk mass changes. The latter are reflective of volcanic processes, involving the dynamics of magma and exsolved gas in the upper part of Mt. Etna's plumbing system. Our results confirm the operational possibilities of quantum gravimetry and open new horizons for the application of the gravity method in geophysics.

Plain Language Summary

Mass redistributions occurring in the Earth's interior, for example when a magma batch is displaced through the feeding system of an active volcano, may induce tiny changes in gravity over time, measurable on the ground. Measurement of such changes requires high-precision devices, namely, the gravimeters, which can detect variations as small as one part in 10^9 of the gravity acceleration on Earth. However, standard gravimeters are not ideally suited for use in harsh field conditions, especially when continuous measurements are the target. Recent advances in quantum technology have allowed the development of a

portable gravimeter which can successfully operate under field conditions. Here we present the world's first application of this quantum gravimeter for monitoring and studying an active volcano. The device was deployed only 2.5 km away from the summit active craters of Mt. Etna volcano (Italy) and has provided a high-quality gravity time series. Inspection of this time series highlighted gravity changes which are reflective of bulk volcanic processes, involving magma and exsolved gas in the upper part of Mt. Etna's plumbing system.

1. Introduction

In recent years, monitoring of subsurface masses, natural or engineered, has become increasingly important. The study of geological reservoirs can address issues related with energy supply, climate change mitigation and the assessment of natural hazards, such as seismicity and volcanic eruptions (Dzurisin, 2003; Thierry et al., 2015; Poland and Anderson, 2020). Understanding aquifer charge and discharge, carbon sequestration and volcanic processes involves multiparametric approaches to inform predictive and simulation models. Gravimetry provides unique direct information on changes in the distribution of underground masses over time (Carbone et al., 2017; Van Camp et al., 2017). It can therefore be utilized to gain insight into the dynamics of subsurface fluids, like water, hydrocarbons, and magma (Chapman et al., 2008; Gasperikova and Hoversten, 2008; Sugihara and Ishido, 2008). However, gravimetry has not been employed extensively, mainly due to stringent instrumental limitations. To address geophysical issues, gravity changes between one part in 10^6 and one part in 10^9 of the standard gravity on Earth ($g = 9.8$ m/s^2) should be precisely measured over timescales between minutes and years and at several locations. This is only marginally compatible with currently available instruments (Van Camp et al., 2017), which are, in general, difficult to utilize in the field, especially under the harsh environmental conditions close to geodynamically active areas (e.g., the active craters of a volcano).

Quantum technologies provide a key to address this challenge. Sensors based on matter-wave interferometry with cold atoms are now reaching a high level of maturity (Geiger et al., 2020). Technological developments have been driven by possible applications in future space missions, which led to experiments with quantum sensors in challenging environments (Geiger et al., 2011; Müntinga et al., 2013; Barrett et al., 2016; Becker et al., 2018). In parallel, the performances of high precision absolute quantum gravimeters were demonstrated in the laboratory (Freier et al., 2016; Gillot et al., 2018; Hu et al., 2013; Wang et al., 2018) and outside laboratories, using transportable prototypes (Bidel et al., 2018; Ménoret et al., 2018; Wu et al., 2019; Bidel et al., 2020; Cooke et al., 2021).

Here, we report on a leap forward in quantum technology, by demonstrating a 4-month time series with a resolution of one part in 10^9 of g, acquired in the summit area of Mt. Etna volcano, through the absolute quantum gravimeter named AQG-B. Data from the AQG-B are compared with data from two superconducting gravimeters, installed at different locations on Mt. Etna (Carbone

et al., 2019). Correlated gravity changes amongst the three time series point to mass changes beneath the summit craters area as the common source.

This is the first time a quantum sensor is used to measure gravity changes driven by volcanic processes. Results prove the maturity of cold-atom gravity sensors for field applications, thus opening the way to new ambitious applications (Carbone et al., 2020).

2. Deployment of the AQG-B at Mt. Etna

The AQG-B, produced by iXblue (formerly Muquans), is packaged in three main modules (Fig. 1A) with reduced size and weight (below 300 L and 40 kg each): (i) a power supply module, managing electrical power and thermal regulation, (ii) the laser system, generating the laser light required to manipulate the atoms, and (iii) the sensor head where the atomic measurements take place. Thanks to thermostatic controls in the laser system and sensor head, the device features an operating temperature range of 0 to 40°C. To ease field operation, the number of connections between the laser system and the sensor head has been reduced to only 4, with a cable (including the optical fiber) length of 15 m. The measurement sequence of the AQG-B includes four main steps, that are repeated at a frequency of 1.85 Hz (Ménoret et al., 2018; see Supporting Information S1).

Mt. Etna is one of the most active and better monitored volcanoes in the world (Cannavò et al., 2019). It has been the site of microgravity measurements with different types of instruments (Carbone et al., 2008; Carbone et al., 2017; Carbone et al., 2019). Only spring gravimeters, which are compact, easily transportable and take little power to work, could be deployed in the close vicinity of the active craters, where the strongest volcano-related gravity changes develop (Carbone et al., 2015). As these instruments suffer from strong instrumental drift, they cannot be used to continuously track gravity changes over intervals longer than a few days. Superconducting gravimeters (SGs) are negligibly affected by instrumental drift and can thus precisely measure gravity changes occurring over time scales of minutes to years. However, they are difficult to transport, setup and, more importantly, require ~1.4 kW of continuous power to work, making them mostly unsuited for installation close to the active structures of tall volcanoes.

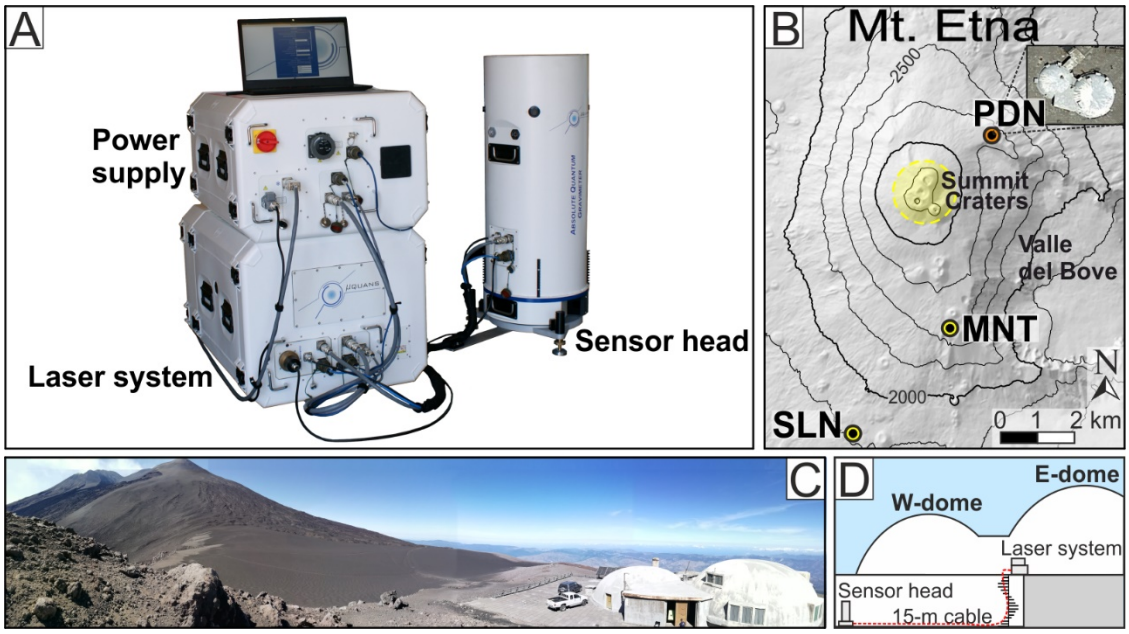

Figure 1 – Deployment of the AQG-B in the summit craters area of Mt. Etna volcano. A: Picture of the AQG-B. The height of the sensor head is 100 cm. B: sketch map of Mt. Etna showing the position of PDN, SLN and MNT stations. The shaded yellow area encloses all the possible horizontal positions of the mass source (Fig. 4 and text). Inset: aerial photo of the PDN observatory (Google Maps). C: panorama looking NW, from the slope to the S of the observatory, showing the proximity of PDN to the summit craters. D: section (not in scale) crossing the observatory and showing the installation configuration of the AQG-B.

In the framework of the NEWTON-g project (Carbone et al., 2020), the AQG-B was deployed close to the summit of Mt. Etna, at the Pizzi Deneri volcanological observatory (PDN; 2800 m elevation, 2.5 km from the summit craters; Fig. 1B and C), for continuous acquisition. The PDN observatory is the closest building to the summit craters of Mt. Etna where long-term continuous gravity measurements can be performed. Nevertheless, harsh environmental conditions (strong daily and seasonal temperature variations, high levels of volcanic tremor, inaccessibility due to snowfall during the months of winter/spring) make the execution of high-precision gravity measurement especially challenging at this location.

The observatory includes two interconnected dome-shaped shelters on the ground floor and a large room in the semi-underground basement (Fig. 1C and D). This room features a concrete pillar that was expressly designed for microgravity measurements. It is directly rooted in the rock underlying the building and detached from the building itself to avoid vibration transmission.

Due to the reduced size of the stairway, only the sensor head of the AQG-B could be installed on the concrete pillar. We used the standard 15-meter cable to connect it to the power supply and laser system, installed on the ground floor (Fig. 1D). As mains electricity is not available, and the site is often unreachable in winter due to snow cover, reliable power supply and data transmission systems are needed to allow for long-term unsupervised operations. In order to provide the continuous electrical power required by the AQG-B (within 500 W), a custom hybrid off-grid power system was installed at PDN. The existing Wi-Fi link of the observatory, managed by INGV-OE, allows for transmission of data and remote operation of the AQG-B through a dedicated software interface.

3. Rejection of volcano-related ground vibrations

The characteristics of seismicity at Mt. Etna, especially in the summit craters zone, are different from those at the quiet sites where gravity measurements are typically performed. In particular, much of the seismic energy is concentrated over the frequency band between 0.1 and 10 Hz (Saccorotti et al., 2004). This frequency range overlaps with the maximum sensitivity of the acceleration transfer function of the AQG-B, which is a low-pass filter with cut-off at $1/2T$ 8 Hz (Geiger et al., 2011). In order to mitigate the effect of ground vibrations, we implement an active compensation system (Lautier et al., 2014). This was initially based on the use of a high-performance classical accelerometer (Nanometrics Titan) integrated in the sensor head (Ménoret et al., 2018). This sensor is particularly well adapted for high frequencies, but the high-pass filters required to remove the DC component of the sensor introduce a significant dephasing at low frequencies, where the amplitude of the signal is high at Mt. Etna.

Simulations based on (i) vibration spectra previously recorded at PDN under different levels of volcanic tremor and (ii) the response functions of both the classical accelerometer and the atom interferometer, showed that, using the standard vibration compensation system, it is not possible to obtain a gravity signal-to-noise ratio compatible with the required performances.

The vibration rejection system was therefore optimized by replacing the accelerometer with a broadband seismometer (Nanometrics Trillium Compact 120s). New simulations showed that, with the improved vibration rejection system, the AQG-B can reach sensitivities between 1200 and 2500 nm/s^2 at 1s, depending on the level of volcanic tremor.

Due to the lower cutoff frequency (around 100 Hz), vibration data acquired through the seismometer are more delayed (~2.5 ms) than data from the accelerometer (cutoff frequency = 430 Hz; delay of around 500 µs), implying that more data are missing when the phase correction is applied to the Raman laser. Combined with a higher sensitivity near the first and last pulses when using the velocity transfer function, this can significantly deteriorate the quality of the real-time compensation. We mitigate this effect by applying a post-correction

to the atomic ratio, corresponding to the residual vibration phaseshift due to the uncompensated delay.

To quantify the efficiency of vibration rejection, we compare the distribution of interferometric phases computed from the seismometer signal and used for real-time compensation to the distribution of phases at the output of the atom interferometer. The resulting rejection efficiency is of the order of 100. In other words, if no active compensation was implemented, phase noise would have a standard deviation of several radians instead of a few tens of milliradians with the active compensation. This is beyond the linear range of the atom interferometer, meaning that, without the active compensation, it would not be possible to recover the value of gravity acceleration unambiguously (Lautier et al., 2014).

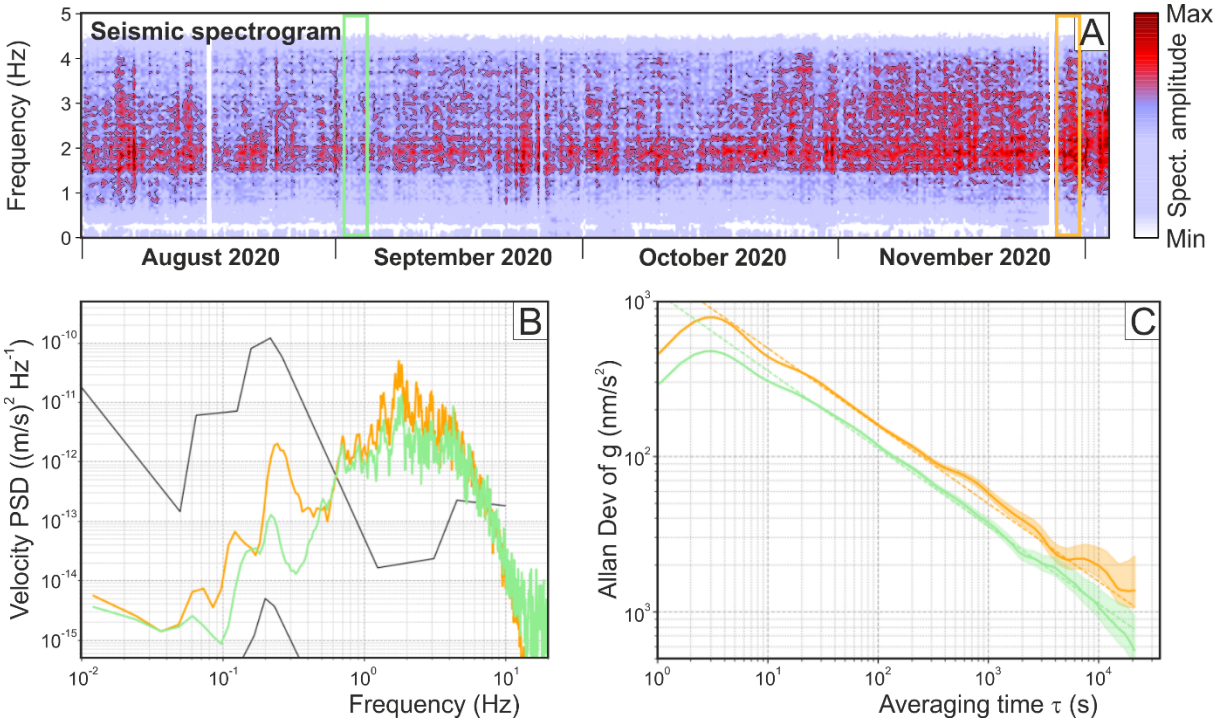

Figure 2 - Sensitivity analysis on data from the AQG-B. A: spectrogram of the vertical-component seismic signal from the Pizzi Deneri station (EPDN; 1 August to 3 December 2020). The green and orange boxes mark periods of low and high volcanic tremor amplitude, respectively. B: Power spectral density (PSD) of the seismic velocity recorded at EPDN, during the phases of low (green) and high (orange) tremor amplitude marked in the spectrogram. Black curves indicate the new high and low noise models from Peterson (1993). C: Allan deviation of the corrected gravity data from the AQG-B at PDN, during the low (green) and high (orange) tremor phases. The green and orange dashed

lines in the Allan plot indicate a sensitivity of 1200 and 1600 nm.s^{-2}.$\tau^{-1/2}$, respectively.

Fig. 2A shows the spectrogram of the vertical component of the seismic signal from PDN during 1 August to 3 December 2020. The green and orange boxes mark two subintervals of low and high tremor, respectively. Power Spectrum Densities of the seismic velocities during the two subintervals are shown in Fig. 2B. Allan deviation analysis (Riley, 2008), performed on the corrected gravity data from the AQG-B at PDN (Fig. 2C), indicates a sensitivity of approximately 1200 and 1600 nm/s^2 at 1 second, for the subintervals of low and high tremor, respectively, corresponding to only a 2 to 3-fold degradation with respect to a quiet laboratory environment (Carbone et al., 2020).These results show the efficiency of the real-time vibration rejection strategy relying on a broadband seismometer and suggest that, even during periods of high volcanic tremor, the data quality is suitable for studying volcano-related gravity changes. Indeed, once data from the AQG-B are averaged over time windows of 1 to 5 hours, it is possible to track gravity changes with amplitudes ranging between a few tens and a few hundreds of nm/s^2, occurring over time scales of days to weeks (see Section 4 and Fig. 3).

4. Results

Gravity data from the AQG-B are corrected for the external perturbing effects driven by Earth tides, polar motion, atmospheric pressure and ground tilt (Fig. S1). While Earth tide and polar motion effects are retrieved through standard models (Van Camp et al., 2017), on-site measurements are required to evaluate the other effects. Data from a barometer fitted to the gravimeter is used to calculate the effect driven by local atmospheric pressure changes (Merriam, 1992). Two high-precision tiltmeters, fitted to the sensor head of the AQG-B, continuously record possible deviations from verticality and the signal they provide is used to correct the gravity signal for possible angular drifts.

The AQG-B recorded gravity data at PDN for ~4 months (1 August to 3 December 2020; Fig. 3A). The gaps in the time series are due to temporary failures of the off-grid power supply system, which caused abrupt shutdowns of the AQG-B. These failures did not damage the instrument, and a remote restart of all the subsystems (ion pump, electronics, lasers) was possible once electrical power was restored. Thanks to the accuracy and repeatability of the AQG-B, no instrumental change in the average level of the signal occurred across any of the above gaps. Furthermore, no significant instrumental drift affects the data from the AQG-B during the studied period.

Residual gravity data from the AQG-B are validated through cross-analysis with data produced by the two iGrav SGs installed on the southern slopes of Mt. Etna (Carbone et al., 2019). Fig. 3B shows the residual gravity signal from iGrav#16, installed in the facilities of the Serra La Nave astrophysical observatory (SLN; Fig. 1B). The signal is corrected for the effects of Earth tide, atmospheric pressure and ground tilt. Thanks to the low-noise characteristics

of SGs and also due to the fact that the instrument is installed relatively far from the active summit area of the volcano (~6.5 km), a precision better than 10 nm/s^2 is obtained after averaging data over a few minutes (Fig. 3B).

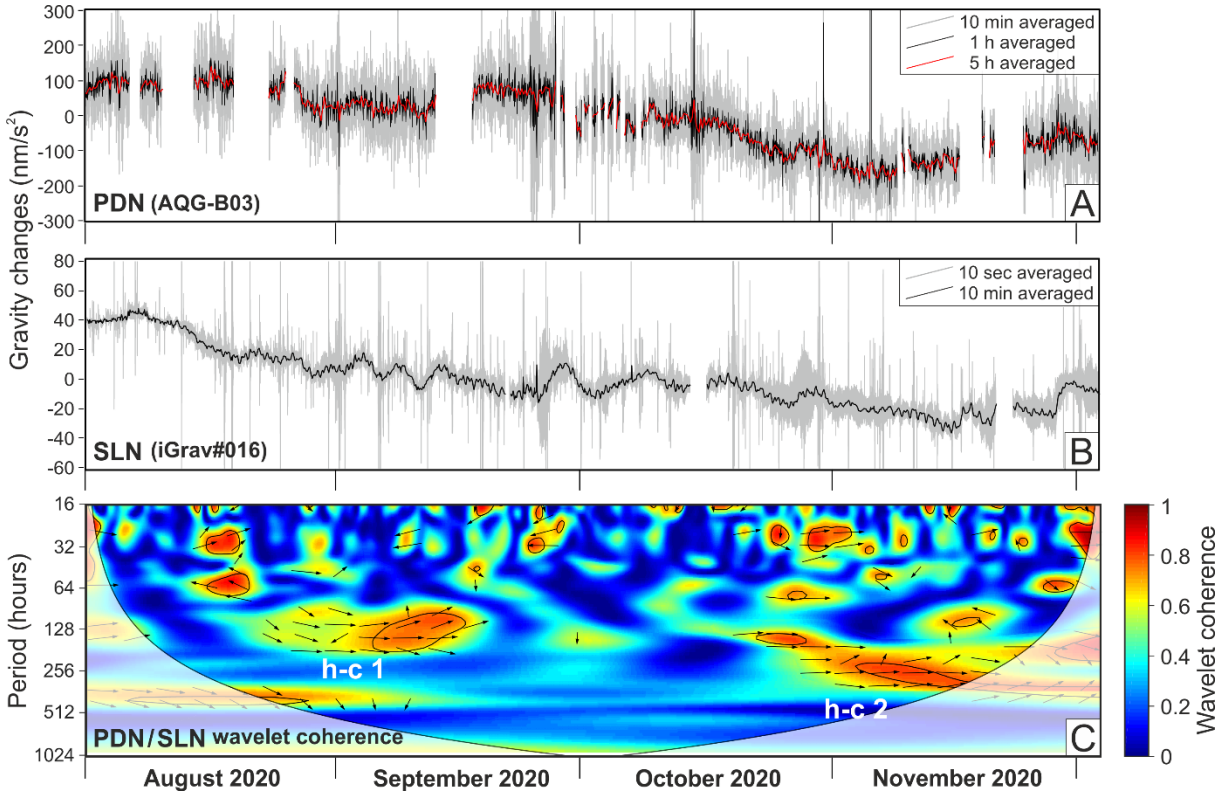

Figure 3 – Gravity time series and wavelet coherence analysis. A: Gravity time series from PDN (1 August to 3 December 2020), after removal of the perturbing effects shown in panels B – F of Fig. S1. Data are averaged over 10-minute (grey curve), 1-hour (black curve) and 5-hour (red curve) intervals. B: Gravity time series from SLN, after removal of Earth tide, atmospheric pressure, ground tilt and polar motion. Data are averaged over 10-second (grey curve) and 10-minute (black curve) intervals. C: Wavelet coherence between the signals in A and B.

To examine the relation between the two gravity time series, we employ the wavelet coherence analysis (Grinsted et al., 2004). This method highlights how coherent the cross-wavelet transform of two time series is and can be thought as a localised correlation coefficient in the time-frequency space.

The wavelet coherence plot (Fig. 3C) indicates, over wavelet scales corresponding to periods longer than 4-5 days, high coherence during two subintervals: late August to mid-September (h-c 1) and mid-October to early November (h-c 2). In both cases, arrows pointing right indicate in-phase behavior. During the first subinterval, weak oscillations over time scales of about 5 days occurred around

an almost constant level of the gravity signal (Fig. 4A). During the second subinterval, an overall gravity decrease was observed (Fig. 4B). For the two subintervals of high coherence, the amplitude ratio between the signals from PDN and SLN is calculated as the slope of the best linear fit between the two time series (Poland and Carbone, 2016). Results point to PDN/SLN amplitude ratios of ~3 and ~6, during the first and second subinterval, respectively (Fig. 4C and D).

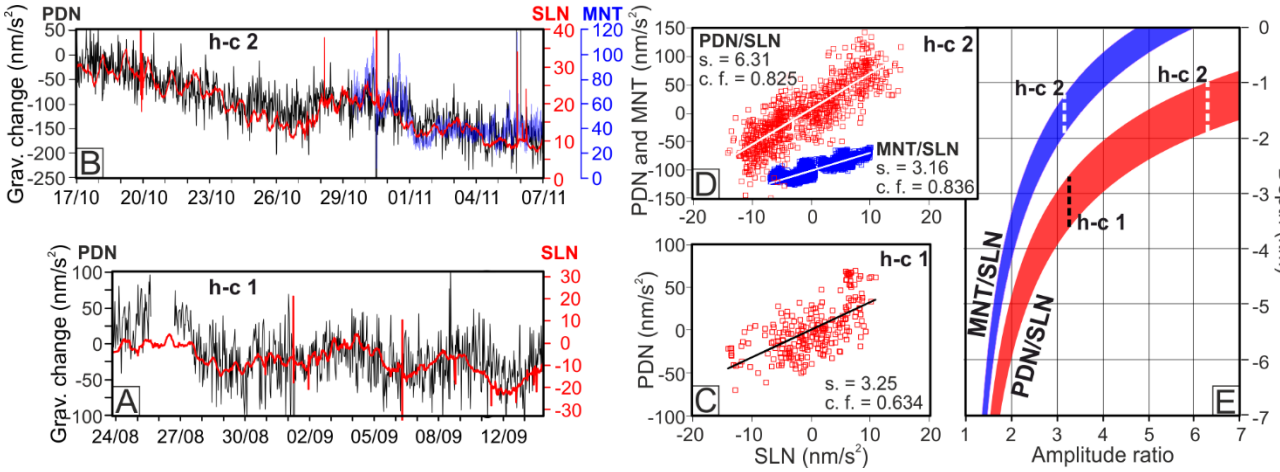

Figure 4 – Gravity time series during high-coherence phases and derivation of mass source depths. A and B: gravity time series from PDN (black curves) and SLN (red curves), during the first (h-c 1) and second (h-c 2) subintervals of high coherence. As for h-c 2, the available signal from MNT is also shown (blue curve in panel B). C and D: Scatterplots of SLN against PDN, during h-c 1, and SLN against PDN and SLN against MNT, during h-c 2. For each scatterplot, the slope of the best-fitting line and the correlation coefficient are reported. E: PDN/SLN (red area) and MNT/SLN (blue area) gravity amplitude ratio versus depth of the mass source. The calculations are performed for all the possible positions of the mass source enclosed in the yellow area of Fig. 1B. Dashed segments mark the values of the observed amplitude ratios during h-c 1 and h-c2.

During the period under study, the other operating SG in the mini-array of Mt. Etna (La Montagnola hut; MNT; Fig. 1B) worked only intermittently, due to problems in the data acquisition system. The available data cover only the last part of the h-c 2 interval and shows a decreasing pattern which is well correlated with the changes observed at PDN and SLN (Fig. 4B). The MNT/SLN amplitude ratio during this interval is ~3 (Fig. 4D).

5. Discussion

Only negligible ground deformation (i.e., within the standard error of GPS data) occurred during the two subintervals of high coherence, thus suggesting that

the observed gravity changes are mostly due to subsurface mass redistributions. Estimations of the depths at which these mass changes occurred are made using the inversion method described by Carbone and Poland (2012; see Support Information S2). Assuming that the horizontal position of the gravity source lies within a ~2-km-wide area enclosing the summit active craters of Etna (Fig. 1B), each value of the gravity amplitude ratio will define a range of possible source depths, as depicted through the red (PDN/SLN) and blue (MNT/SLN) areas of Fig. 4E. Accordingly, the ~3 PDN/SLN amplitude ratio during h-c 1 points to a depth of the mass source of between 2.5 and 3.5 km b.s.l.. Conversely, the PDN/SLN (~6) and MNT/SLN (~3) amplitude ratios during h-c 2 consistently indicate a shallower mass source at 1 – 2 km b.s.l.

The couplings between the signal from the AQG-B and the signals acquired through SGs installed at sites 5 (MNT) and 9 (SLN) km away from PDN (Fig. 1B) prove that, during the period under study, the AQG-B measured gravity changes reflective of bulk mass redistributions, rather than local and/or instrumental effects. Furthermore, the estimated source depths (Fig. 4E) are in agreement with the results of previous studies (Carbone et al., 2003; Carbone et al., 2019), thus suggesting that volcanic processes are behind the causative mass changes.

The gravity oscillations during h-c 1 are likely reflective of transient mass changes (on the order of 10^{10} kg), possibly related to the pulsating ascent of gas-rich fluids towards the intermediate and shallow portions of the magmatic system (Paonita et al., 2021). The upward flushing of this fluid phase (Ferlito, 2018) is thought to control the occurrence and intensity of explosive activity at Mt. Etna (Moretti et al., 2018), implying that tracking it is important from the standpoint of volcano monitoring. Detection techniques based on geochemical measurements may fail to recognize the surface signature of this process, especially if it consists of minor gas emissions from the plume and from the flanks of the volcano, occurring over relatively short time scales (e.g., a few days, as in the case of changes during h-c 1). In that sense, cross analysis with high-precision continuous gravity measurements provides a powerful tool to assess a more reliable picture of the volcano's state of activity.

The gravity decrease phase throughout h-c 2, corresponding to a mass decrease of about $5*10^{10}$ kg, could indicate a gradual increase in the proportion of exsolved gas to magma in a shallower portion of the volcano's plumbing system. Early recognition of gas segregation processes at active volcanoes is of upmost importance, given the implications that local accumulations of volatiles may have for the development of energetic and potentially dangerous paroxysms (Allard et al., 2005; Carbone et al., 2008).

A decrease in the flux of SO_2 emitted by Mt. Etna's plume (from about 4000 to about 2000 tons/day) was observed during the first half of October (INGV-OE, 2020). Low degassing values persisted throughout the whole h-c 2 interval, while the SO_2 flux started increasing again since late-November. The phase of gravity decrease and low gas emission rate may have resulted from rheological

stiffening in the upper conduits (Nadeau et al., 2011), inhibiting gas discharge and favoring accumulation at shallow depth. Cooling of the magma that fed mild Strombolian activity at two out of the four summit craters of Mt. Etna, during September and October 2020 (INGV-OE, 2020), could have led to the formation of the inferred stiffened layer. Also in this case, we show the importance of cross-checking geochemical observation with continuous gravity measurements: without the information from gravimetry, it is not possible to tell whether the observed decrease in the gas flux from the craters was due either to a lower supply from below, or to a reduced ability of the upper plumbing system to discharge the available gas.

6. Conclusive remarks

With respect to instruments that have been previously utilized for continuous gravity measurements under harsh environmental conditions, the AQG-B has shown several advantages. It provides driftless measurements, allowing to precisely track changes over time-scales of days to months. Indeed, it would not have been possible to detect a gravity change like the one during the h-c 2 interval using a spring gravimeter, because of the marked nonlinear drift over periods longer than a few days (Carbone et al., 2017). Furthermore, thanks to the accuracy of the AQG-B, no fictitious changes in the level of the signal occur across gaps in the time series. Such "jumps" may occur when relative instruments are employed (spring meters and SGs), requiring arbitrary adjustments to compensate for changes in the baseline, that may eventually lead to wrong inferences about the driving processes.

Although the AQG-B features a lower short-term precision than the iGrav SG, it takes ~1/3 of the continuous power supply needed by that device, which allows for installation at sites with no mains electricity supply. The AQG-B is also easier to install and maintain than the iGrav, thanks to the lack of cryogenics and related equipment. Furthermore, inspection of the time series from the AQG-B at PDN did not reveal the occurrence of apparent changes resulting from the instrumental response to inertial forces, which were found in the signal from the iGravs at Mt. Etna, during phases of strong volcanic tremor (Carbone et al., 2019).

Field gravimetry is a relatively new area of application for quantum technology and there are ongoing improvements, both in terms of power consumption and of size and transportability of the instrumentation.

Cross analysis of the time series from the AQG-B and the iGravs at Mt. Etna revealed the occurrence of gravity changes likely driven by bulk volcanic processes. In particular, we propose that changes in the relative proportions of magma and exsolved gas in the upper part of the volcano's feeding system triggered the observed gravity changes.

Our successful demonstration of a quantum sensor based on atom interferometry opens new horizons not only for volcano gravimetry, but also for the application of the gravity method to contexts where reliable field measurements in hostile

environments may be required, such as the study of groundwater dynamics, geothermal energy systems and carbon sequestration.

Acknowledgments

We thank the technical, administrative and scientific Muquans / iXblue staff for their work and support. We also acknowledge the INGV-OE technical and scientific staff for their support in maintaining the facilities at the PDN observatory and for making available the seismic data used in the present study. These data are not publicly available, access can be requested from `ufs.ct@ingv.it` .

This work was supported by the NEWTON-g project, which has received funding from the EC's Horizon 2020 programme, under the FETOPEN-2016/2017 call (Grant Agreement No 801221).

BD, VM, LAM and JLG declare the following competing interests: iXblue (formerly Muquans) is a privately held company. BD, VM, LAM and JLG are employed by iXblue and hold shares in the company.

References

Allard, P., Burton, M. & Murè, F. (2005). Spectroscopic evidence for a lava fountain driven by previously accumulated magmatic gas. *Nature*, *433*, 407–410.

Barrett, B., Antoni-Micollier, L., Chichet, L., Battelier, B., Lévèque, T., Landragin, A. & Bouyer, P. (2016). Dual matter-wave inertial sensors in weightlessness. *Nature Communications*, *7*, 13786.

Becker, D., Lachmann, M. D., Seidel, S. T., Ahlers, H., Dinkelaker, A. et al. (2018). Space-borne Bose–Einstein condensation for precision interferometry. *Nature*, *562*, 391–395.

Bidel, Y., Zahzam, N., Blanchard, C., Bonnin, A., Cadoret, M., Bresson, A., Rouxel, D. & Lequentrec-Lalancette, M. F. (2018). Absolute marine gravimetry with matter-wave interferometry. *Nature Communications*, *9*, 627.

Bidel, Y., Zahzam, N., Bresson, A., Blanchard, C., Cadoret, M., Olesen, A. V. & Forsberg, R. (2020). Absolute airborne gravimetry with a cold atom sensor. *Journal of Geodesy*, *94*, 20.

Cannavò, F., Sciotto, M., Cannata, A. & Di Grazia, G. (2019). An integrated geophysical approach to track magma intrusion: The 2018 Christmas eve eruption at Mount Etna. *Geophysical Research Letters*, *46*, 8009–8017.

Carbone, D., Budetta, G. & Greco, F. (2003). Possible mechanisms of magma redistribution under Mt Etna during the 1994–1999 period detected through microgravity measurements. *Geophysical Journal International*, *153*, 187–200.

Carbone, D., Zuccarello, L. & Saccorotti, G. (2008). Geophysical indications of magma uprising at Mt. Etna during the December 2005 to January 2006 non-eruptive period. *Geophysical Research Letters*, *35*(6), L06305.

Carbone, D. & Poland, M. P. (2012). Gravity fluctuations induced by magma convection at Kīlauea Volcano, Hawai'i. *Geology*, *40*(9), 803–806.

Carbone, D., Zuccarello, L., Messina, A., Scollo, S. & Rymer, H. (2015). Balancing bulk gas accumulation and gas output before and during lava fountaining episodes at Mt. Etna. *Scientific Reports*, *5*, 18049.

Carbone, D., Poland, M. P., Diament, M. & Greco, F. (2017). The added value of time-variable microgravimetry to the understanding of how volcanoes work. *Earth-Science Reviews*, *169*, 146-179.

Carbone, D., Cannavò, F., Greco, F., Reineman, R. & Warburton, R. J. (2019). The benefits of using a network of superconducting gravimeters to monitor and study active volcanoes. *Journal of Volcanology and Geothermal Research*, *124*, 4035–4050.

Carbone, D. et al. (2020). The NEWTON-g Gravity Imager: Toward New Paradigms for Terrain Gravimetry. *Frontiers in Earth Science*, *8*, 573396.

Chapman, D. S., Sahm, E. & Gettings, P. (2008). Monitoring aquifer recharge using repeated high-precision gravity measurements: A pilot study in South Weber, Utah. *Geophysics*, *73*(6), WA83-WA93.

Cooke, A.-K., Champollion, C. & Le Moigne, N. (2021). First evaluation of an absolute quantum gravimeter (AQG#B01) for future field experiments. *Geoscientific Instrumentation, Methods and Data Systems*, *10*, 65–79.

Dzurisin, D. (2003). A comprehensive approach to monitoring volcano deformation as a window on the eruption cycle. *Reviews of Geophysics*, *41*(1), 1001.

Ferlito, C. (2018). Mount Etna volcano (Italy). Just a giant hot spring! *Earth-Science Reviews*, *177*, 14–23.

Freier, C., Hauth, M., Schkolnik, V., Leykauf, B., Schiling, M., Wziontek, H., Scherneck, H. G., Müller J. & Peters, A. (2016). Mobile quantum gravity sensor with unprecedented stability. *Journal of Physics: Conference Series*, *723*, 012050.

Gasperikova, E. & Hoversten, G. M. (2008). Gravity monitoring of CO2 movement during sequestration: Model studies. *Geophysics, 73*(6), WA105-WA112.

Geiger, R., Ménoret, V., Stern, G., Zahzam, N., Cheinet, P., Battelier, B., Viling, A., Moron, F., Lours, M., Bidel, Y., Bresson, A., Landragin, A. & Bouyer, P. (2011). Detecting inertial effects with airborne matter-wave interferometry. *Nature Communications*, *2*, 474.

Geiger, R., Landragin, A., Merlet, S. & Pereira Dos Santos, F. (2020). High-accuracy inertial measurements with cold-atom sensors. *AVS Quantum Science*, *2*, 024702.

Gillot, P., Francis, O., Landragin, A., Pereira Dos Santos, F. & Merlet, S. (2014). Stability comparison of two absolute gravimeters: optical versus atomic

interferometers. *Metrologia*, *51*, L15.

Grinsted, A., Moore, J. C. & Jevrejeva, S. (2004). Application of the cross wavelet transform and wavelet coherence to geophysical time series. *Nonlinear Processes in Geophysics*, *11*, 561–566.

Hu, Z.-H., Sun, B.-L., Duan, X.-C., Zhou, M.-K., Chen, L.-L., Zhan, S., Zhang, Q.-Z. & Luo, J. (2013). Demonstration of an ultrahigh-sensitivity atom-interferometry absolute gravimeter. *Physical Review A*, *88*, 043610.

INGV-OE (2020). Bollettino settimanale sul monitoraggio vulcanico, geochimico e sismico del vulcano Etna del 22/12/2020. https://www.ct.ingv.it/index.php/monitoraggio-e-sorveglianza/prodotti-del-monitoraggio/bollettini-settimanali-multidisciplinari

Lautier, J., Volodimer, L., Hardin, T., Merlet, S., Lours, M., Pereira Dos Santos, F. & Landragin, A. (2014). Hybridizing matter-wave and classical accelerometers. *Applied Physics Letters*, *105*, 144102.

Ménoret, V., Vermeulen, P., Le Moigne, N., Bonvalot, S., Bouyer, P., Landragin, L. & Desruelle, B. (2018). Gravity measurements below 10^{-9} g with a transportable absolute quantum gravimeter. *Scientific Reports*, *8*, 12300.

Merriam, J. B. (1992). Atmospheric pressure and gravity. *Geophysical Journal International*, *109*(3), 488–500.

Moretti, R., Métrich, N., Arienzo, I., Di Renzo, V., Aiuppa, A. & Allard, P. (2018). Degassing vs. eruptive styles at Mt. Etna volcano (Sicily, Italy). Part I: Volatile stocking, gas fluxing, and the shift from low-energy to highly explosive basaltic eruptions. *Chemical Geology*, *482*, 1–17.

Müntinga, H., Ahlers, H., Krutzik, M., Wenzlawski, A., Arnold S. et al. (2013). Interferometry with Bose-Einstein condensates in microgravity. *Physical Review Letters*, *110*, 093602.

Nadeau, P. A., Palma, J. L. & Waite, G. P. (2011). Linking volcanic tremor, degassing, and eruption dynamics via SO_2 imaging, *Geophysical Research Letters*, *38*, L01304.

Paonita, A., Liuzzo, M., Salerno, G., Federico, C., Bonfanti, P., Caracausi, A., Giuffrida, G., La Spina, A., Caltabiano, T., Gurrieri, S. & Giudice, G. (2021). Intense overpressurization at basaltic open-conduit volcanoes as inferred by geochemical signals: The case of the Mt. Etna December 2018 eruption. *Science Advances*, *7*, eabg6297.

Peterson, J. R. (1993). Observation and modeling of seismic background noise. *U.S. Geological Survey report*, *93*(322). http://pubs.er.usgs.gov/publication/ofr93322

Poland, M. P. & Carbone, D. (2016). Insights into shallow magmatic processes at Kīlauea Volcano, Hawai'i, from a multiyear continuous gravity time series. *Journal of Geophysical Research - Solid Earth*, *121*(7), 5477–5492.

Poland, M. P. & Anderson, K. R. (2020). Partly cloudy with a chance of lava flows: Forecasting volcanic eruptions in the twenty-first century. *Journal of Geophysical Research - Solid Earth*, 125, e2018JB016974.

Riley, W. J. (2008). Hanbook of frequency stability analysis. *NIST special publication*, *1065*, https://tf.nist.gov/general/pdf/2220.pdf

Saccorotti, G., Zuccarello, L. Del Pezzo, E., Ibanez, J. & Gresta, S. (2004). Quantitative analysis of the tremor wavefield at Etna Volcano, Italy. *Journal of Geophysical Research - Solid Earth*, *136*, 223–245.

Sugihara, M. & Ishido, T. (2008). Geothermal reservoir monitoring with a combination of absolute and relative gravimetry. *Geophysics*, *73*(6), WA37–WA47.

Thierry, P., Neri, M., Le Cozannet, G., Jousset, P. & Costa, A. (2015). Preface: Approaches and Methods to Improve Risk Management in Volcanic Areas. *Natural Hazards and Earth System Sciences*, *15*, 197–201.

Van Camp, M., de Viron, O., Watlet, A., Meurers, B., Francis, O. & Caudron, C. (2017). Geophysics from terrestrial time-variable gravity measurements. *Reviews of Geophysics*, *55*, 938-992.

Wang, S.-K., Zhao, Y., Zhuang, W., Li, T.-C., Wu, S.-Q., Feng, J.-Y. & Li, C.-J. (2018). Shift Evaluation of the atomic gravimeter NIM-AGRb-1 and its comparison with FG5X. *Metrologia*, *55*, 360.

Wu, X., Pagel, Z., Malek, B. S., Nguyen, T. H., Zi, F., Scheirer, D.S. & Müller, H. (2019). Gravity surveys using a mobile atom interferometer. *Science Advances*, *5*, 9, eaax0800.